2021 43rd Annual International Conference of the
IEEE Engineering in Medicine & Biology Society (EMBC)
Oct 31 - Nov 4, 2021. Virtual Conference

Direct Myoelectric Control Modifies Lower Limb Functional Connectivity: A Case Study

Wentao Liu, Aaron Fleming, I-Chieh Lee, and He (Helen) Huang

Abstract— **Prostheses with direct EMG control could restore amputee's biomechanics structure and residual muscle functions by using efferent signals to drive prosthetic ankle joint movements. Because only feedforward control is restored, it is unclear 1) what neuromuscular control mechanisms are used in coordinating residual and intact muscle activities and 2) how this mechanism changes over guided training with the prosthetic ankle. To address these questions, we applied functional connectivity analysis to an individual with unilateral lower-limb amputation during postural sway task. We built functional connectivity networks of surface EMGs from eleven lower-limb muscles during three sessions to investigate the coupling among different function modules. We observed that functional network was reshaped by training and we identified a stronger connection between residual and intact below knee modules with improved bilateral symmetry after amputee acquired skills to better control the powered prosthetic ankle. The evaluation session showed that functional connectivity was largely preserved even after nine months interval. This preliminary study might inform a unique way to unveil the potential neuromechanic changes that occur after extended training with direct EMG control of a powered prosthetic ankle.**

I. INTRODUCTION

Powered lower-limb prostheses with direct neural control allows amputees to generate control signals using residual muscles, in which the electromyography (EMG) signals collected from residual muscles are mapped into ankle joint parameters to the prosthetic joint continuously in real time [1]. Since this control is directly linked with descending neural commands from the amputee, it offers the ability to restore function of a wide range of activities otherwise impossible with a passive prosthetic ankle joint. Recent studies have shown benefits in improved postural control and stability over a range of tasks over the course of guided, extended training [2]. However the neural connectivity changes within the residual muscles and between intact and residual muscle groups during training remains unknown. It is also unclear how neural mechanisms behind improved residual muscle activity might change over a long period of disuse. Specifically, we seek in this preliminary study to 1) understand the neuromuscular control mechanisms behind residual and intact muscles coordination and 2) investigate whether improved prosthetic ankle function is a result of short-term adaptation or long-term learned behavior.

This work was funded by National Science Foundation (NSF1954587) and National Institutes of Health (NICHD F31HD101285).

Authors are with UNC/NC State Joint Department of Biomedical Engineering, NC State University, Raleigh, NC, 27695; University of North Carolina at Chapel Hill, Chapel Hill, NC 27599.

Corresponding author: Wentao Liu (e-mail: wtliu@unc.edu)

For this investigation of the neural mechanisms during learning of direct EMG control of a powered prosthetic ankle, we utilized network analysis. The frequency spectrum patterns extracted from EMG by this method indicate potential neural pathways. The weights of different groupings of muscles reflect their connection patterns [3], [4]. We collected the surface EMG from an amputee performing postural sway task while using direct EMG control of a powered prosthetic ankle. The topology features of multi-muscle coordination and the movement outcome in pre-training, post-training and a retention session after nine months were compared. Based on our knowledge, this is the first paper to apply network analysis to capture the potential neuro re-mapping during training with direct EMG control with a long retention design to assess preservation of neural function. The results of this study may inform potential advantage of powered ankle prosthesis with direct myoelectric control and benefit many researches in understanding the neuromechanics of lower-limb amputee.

II. MATERIALS AND METHODS

A. Experimental Protocol and Participant

One unilateral, below-knee amputee participated the study after providing institutionally-approved informed consent. The participant is an active community ambulator (K3), 31 years old, 90.7kg, 13 years post-amputation (trauma). Participant was trained with the neural prosthesis control for three sessions. After 9 months the participant returned for an additional evaluation session.

During training and evaluation days, the participant completed a postural sway task (Fig. 1) [5]. We asked the participant to sway as far forward and backward as possible, while following audio cues via a metronome at a rate of 30 BPM for a total of 25 sways. We conducted a minimum of 4 postural sway trials per day, and a maximum of 8 trials. Over all training days the participant trained with the device a total of 4.5 hours.

B. Data Acquisition, Device, and Preprocessing

From training and evaluation days we extracted 3 sessions for further analysis: 1) Pre-training stage (the subject was naive about the device), 2) Post-training stage (the last session for learning the control of device), 3) Retention stage (9 months after post-training). We selected the first trial from each of these sessions for further evaluation to avoid any effects that may arise from muscle fatigue. During each trial the participant stood upright on an instrumented split-belt

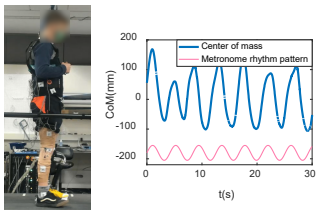

Fig. 1. (a) The experiment setup. (b) Center of mass during the postural sway task in retention session as a representative. Only half minute of data was shown in here, together with the rhythm pattern of metronome as a reference. The Y axis only applies to the center of mass. The participant was asked to try his best to follow the 30 BPM rhythm.

treadmill (1000Hz, Bertec) and we collected full-body kinematics using Vicon 3D motion capture. We collected muscle activity using EMG sensors over intact muscles (Motion Lab MA-420, Gainx20) (Fig. 2). For residual muscles in below knee region, TA and GAS, we used thin, neo-natal EMG sensors (Neuroline 715, 1mm thickness) routed to a pre-amplifier (Motion Lab MA-412, Gainx20) taking care to avoid bony landmarks inside the prosthetic socket interface. We used alternate sensors for residual muscle activities due to their low-profile in the prosthetic socket.

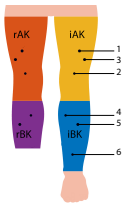

	Muscle	Abbreviation
1	Rectus femoris	RF
2	Biceps femoris	BF
3	Vastus lateralis	VL
4	Tibialis anterior	TA
5	Gastrocnemius	GAS
6	Soleus	SOL

Fig. 2. The functional modules and list of muscles of lower-limb. Four modules were identified, which are above knee on the residual limb (rAK, orange area), below knee muscles on residual limb (rBK, purple area), above knee muscles on the intact limb (iAK, yellow area), and below knee muscles on the intact limb (iBK, blue area). The anterior muscle locations are marked with hexagons, and posterior muscle locations are marked with circles.

The participant conducted all sessions with proportional myoelectric control of a pneumatic-actuated prosthetic ankle system. The details of this device can be found in [1]. To generate a control signal for the pneumatic ankle, we processed EMG activity in real time from the residual TA and GAS muscles and gained the smoothed control signal such that a maximum contraction would results in a control signal of 9-10V for each muscle. We used this control signal to proportionally modulate air pressure within the antagonistic pneumatic artificial muscles to drive plantar and dorsiflexion torques. Details on this control system can be found in [2].

For EMG signals collected from all muscles, we applied a 60Hz notch filter to remove the potential power line interference, then used a high pass filter (4th order, Butterworth, 20Hz cut-off) to remove noise and prevent aliasing. EMG envelopes were extracted with Hilbert transform [4].

C. Functional Muscle Network

1) Intermuscular EMG coherence: We calculated pairwise intermuscular coherence $C_{xy}(f)$ for all EMG envelops using

$$C_{xy}(f) = \frac{|\Phi_{xy}(f)|^2}{\Phi_{xx}(f)\Phi_{yy}(f)} \tag{1}$$

where $\Phi_{xy}(f)$ denotes the cross-spectrum between two channels of EMGs, x and y. $\Phi_{xx}(f)$ and $\Phi_{yy}(f)$ are the self-spectrum for the individual channels. The spectral density was estimated using Welch's averaged modified periodogram method with hamming window (0.256s window length) and 50 % of overlap. The intermuscular EMG coherence between all 55 muscle pairs were estimated.

2) Non-negative matrix factorization: Non-negative matrix factorization (NNMF) was adopted to factorize the coherence matrix into distinct frequency components and their corresponding coefficients. It has been applied in a wide range of studies including muscle synergy extraction and spectral demodulation [6]. Compared with other factorization methods, NNMF distinguish itself by yielding nonnegative features which would help with data interpretability [7].

The coherence map C is an $f \times p$ matrix, where f indicates the frequency spectrum and p is the number of muscle pairs which equals 55 in this study. The NNMF factors matrix C into two non-negative matrices W and H. W with dimension of $f \times k$ reflects spectral basis pattern, and H is an $k \times p$ matrix which indicates the corresponding coupling strength under the spectral basis. We used alternating least-squares (ALS) method for the calculation. The rank of factors k was chosen as 3 to maintain variance accounted for (VAF) above 95% for the three sessions.

3) Network analysis for amputee: We grouped recorded muscles into four modules according to its spatial distribution across the low-limbs (Fig. 2). Based on the primary function, each bi-articular muscle was assigned into the region where it has stronger effective lever arm. The GAS, TA, SOL muscles were grouped as below knee modules for each limb, and the VL, RF, BF muscles were grouped as above knee modules. SOL was missing in the residual below knee module.

For network analysis, we built undirected weighted networks to describe functional connection between modules. We characterize functional connectivity of lower-limb muscles through its topology under corresponding frequency components. The within module density, symmetric relations between nodes, and weighted edge in the graph can be used to identify different connection patterns.

Let N denote the size of a local network, which refers to the number of muscles within a functional module. Let E be the observed edges within the module. The within module density is defined as

$$D = \frac{2E}{N(N-1)} \tag{2}$$

which indicated the portion of observed edges in all possible connections of an undirected network of size N. If we assume m elements in module A and n elements in module B, the edge weight between two modules is calculated by

$$\Omega_{AB} = \sum_{i=1}^{m}\sum_{j=1}^{n} h_{ij} \tag{3}$$

where h is the reconstructed weight matrix for the corresponding frequency component according to the muscle index. Intra module connection Ω is a liner combination of weights between all the elements between two modules.

III. RESULTS

Three separate frequency components were extracted for each session (Fig. 3a), the resulting spectral basis pattern, although slightly different from each other, revealed similar components, which are low-range frequency (below 8Hz), mid-range frequency (8-12Hz), and high-range frequency (above 12Hz). We set a threshold for the coupling strength matrix H to eliminate the potential influence of noise (the relative threshold is the median value under corresponding component) and to obtain a network with only significant connections.

The reconstructed clustering graph (Fig. 3b) reflects the functional connectivity in lower-limb. Under the low-range frequency component (component 1), all modules were fully connected across the three evaluated sessions. The within module density did not show a stable pattern. Under the mid-range frequency components (component 2), the rBK had higher within module density compare to others. Similar to the first component, we observed a fully connected network between all modules across all sessions. We observed noticeable differences in the graph structure of the high-range frequency components (component 3). For pre-training, the strongest edges all connected to the intact below knee module. For post-training and retention, the network structure became more balanced compared to pre-training, showing that there was a graduate transition to bilateral connections between below knee modules with the training went on. The coupling between rBK and iBK modules became the dominant connection in post-training and retention sessions.

The participant performance improved with training and was able to fully follow the metronome in the latter two sessions (Fig. 3c). The standard deviation of center of pressure (CoP) became larger for both sides and its standard deviation difference between residual limb and intact limb decreased during post-training, and this behavior was also demonstrated during the retention session 9 months after training (Table I). The standard deviation difference between residual limb and intact limb decreased showing the improvement of symmetry.

TABLE I
STANDARD DEVIATION OF COP FROM INTACT AND RESIDUAL SIDE

Session	SD intact	SD residual	SD difference (mm)
Pre-training	69.55	41.23	28.31
Post-training	73.65	58.64	15.01
Retention	72.87	84.63	11.76

IV. DISCUSSIONS AND CONCLUSIONS

We applied multi-muscle network analysis to the EMG acquired from intact and residual leg muscles during a postural sway task with direct EMG control prosthesis to gain new insight into the potential neural mechanisms behind changes in kinematics and functional connectivity.

Three major components derived from intermuscular coherence indicate different functional connectivity patterns during the amputee participant conducting the postural sway tasks. Low frequency components are strongly shaped by anatomical constraints and kinematics of musculoskeletal system since muscles act as low-pass filter for neuronal inputs, and the influence of motor neural system are expected to be pronounced in the middle and high frequency components [4], [8], [9].

Results from three sessions indicate functional connectivity containing features that changed over short and long time periods. The network structure of functional area (Fig. 3b) illustrated connection changes under the 3rd component, which covers higher frequency range including beta (15–30Hz) and low-gamma band (30–60Hz). We observed an unbalanced pattern in pre-training (stronger connections within intact side modules), and a balanced pattern in post-training and retention (strong intact-residual shank connection). Previous studies postulated that component within this range might be predominantly driven by the primary motor cortex, and this frequency have been identified in periodically modulated movements [10], [11]. Noted that the weights were normalized within every graph in Fig. 3b, so each thick stroke in the network of 3rd component during pre-training indicted that each edge connected to iBK module almost took one third of overall value, and during post-training and retention the coupling between rBK and iBK took almost 100% of overall value. This finding indicates residual muscles potentially engaged in the process of primary motor cortex control, likely sharing the same neural inputs as homologous muscles group on the intact side. Future studies are needed to examine this explanation. Looking into low and middle frequency components we observed similarities exist in network structure across all sessions. This is no surprise since the participant was able to follow the same protocol and produce similar kinematics during postural sway for all sessions, and thus the anatomical constrains and kinematics should be similar for low frequency components. We identified resemblance in alpha band (8–12Hz) across three sessions, which is covered mainly by the middle frequency component. This band has been widely identified in multiple intermuscular coherence studies, and could be an indicator of the formation of functional muscle collectives [12], [13].

The changes in motor control may be reflected in changes in the CoP. Interestingly we found transition from asymmetric to symmetric pattern in CoP trajectories (Fig. 3c), similar to what we observed in network structures. The participant heavily relied on the intact side to bring the body back and forth, as evidenced in part by larger intact CoP excursions than residual side during the pre-training session. The asymmetry in CoP indicates a likely imbalance between bilateral ankle joint contributions. After the participant trained with the direct EMG control of the prosthetic ankle, the bilateral CoP showed a more symmetrical pattern on similar scale in both post-training and retention sessions.

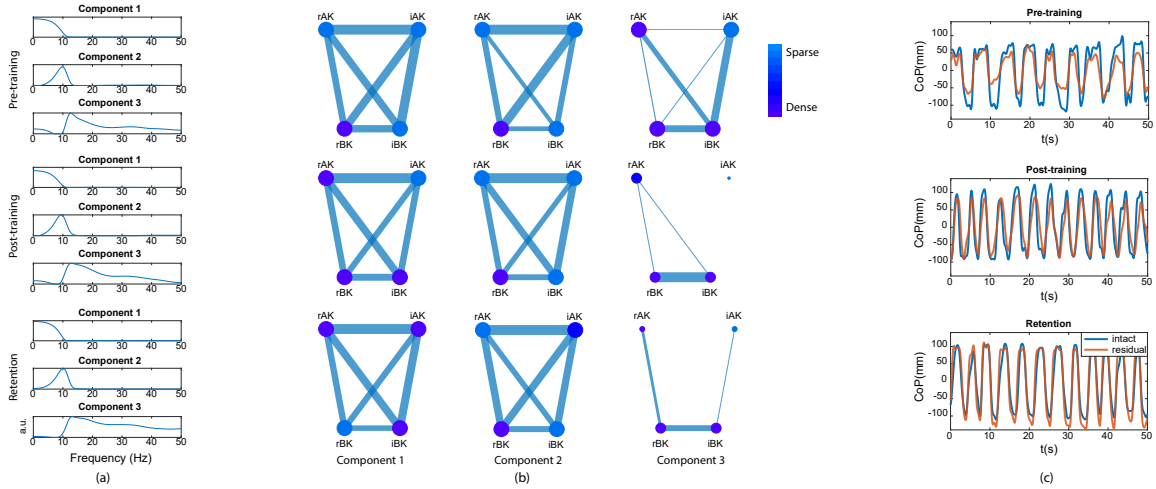

Fig. 3. The extracted components and its corresponding functional network structure, as well as CoP trajectories from pre-training, post-training and retention sessions. (a) Frequency spectra of three components for each training session, which covers low, middle, high frequency range separately. (b) Clustering graph of functional areas in lower-limb. Each row represents a training session, and each column corresponds to a frequency component. The node color represents the local network density within the functional area as described in equation (2). The circle size indicates the degree of the corresponding node, which is described in terms of the number of neighbors that connect to it. The edge width represents the weighted connectedness between areas as described in equation (3). In each graph the weight values were normalized. (c) Bilateral CoP during each session. 50 seconds of representative data were selected. The data were low-pass filtered and the mean values were removed to make the trajectories zero-centered.

Results of improved symmetry between intact and prosthetic ankle joint demonstrate the ability for amputee to learn to coordinate residual TA and GAS, which were previously an antagonistic pair, to restore function of the prosthetic ankle joint. We have observed similar result in previous study [2].

There is a resemblance between post-training and retention session in both network structure and CoP pattern, showing that similar control strategy retained in amputee's behavior and functional connectivity during the postural sway trials. After a 9-months break, the participant was still able to recruit and apply the learned skills immediately. This demonstrates that these behaviors were likely learned rather than a result of short-term adaptation. In addition, this finding could be an evidence for functional neuroplasticity showing that the bilateral coupling between muscles on intact and residual side has been restored and preserved in the participant after training with direct EMG control of a powered prosthetic ankle.

We revealed potential link in biomechanical measurements and neural connectivity structure and demonstrated that network analysis for multi-muscle analysis can potentially unveil the neuroplasticity in postural control with direct myoelectric control prostheses. It will benefit many researches in understanding the neuromechanics of lower-limb amputee. Our future study building upon this work may be used to further explore the effects of novel prosthetic technology on human neuromuscular control.

REFERENCES

[1] S. Huang, J. P. Wensman, and D. P. Ferris, "An Experimental Powered Lower Limb Prosthesis Using Proportional Myoelectric Control," *Journal of Medical Devices*, vol. 8, no. 2, 03 2014.

[2] A. Fleming, S. Huang, E. Buxton, F. Hodges, and H. H. Huang, "Direct continuous electromyographic control of a powered prosthetic ankle for improved postural control after guided physical training: A case study," *Wearable Technologies*, vol. 2, p. e3, 2021.

[3] A. C. Murphy, S. F. Muldoon, D. Baker, A. Lastowka, B. Bennett, M. Yang, and D. S. Bassett, "Structure, function, and control of the human musculoskeletal network," *PLoS biology*, vol. 16, no. 1, p. e2002811, 2018.

[4] J. N. Kerkman, A. Daffertshofer, L. L. Gollo, M. Breakspear, and T. W. Boonstra, "Network structure of the human musculoskeletal system shapes neural interactions on multiple time scales," *Science advances*, vol. 4, no. 6, 2018.

[5] A. Danna-dos Santos, K. Slomka, V. M. Zatsiorsky, and M. L. Latash, "Muscle modes and synergies during voluntary body sway," *Experimental Brain Research*, vol. 179, no. 4, pp. 533–550, 2007.

[6] M. F. Rabbi, C. Pizzolato, D. G. Lloyd, C. P. Carty, D. Devaprakash, and L. E. Diamond, "Non-negative matrix factorisation is the most appropriate method for extraction of muscle synergies in walking and running," *Scientific reports*, vol. 10, no. 1, pp. 1–11, 2020.

[7] D. D. Lee and H. S. Seung, "Learning the parts of objects by non-negative matrix factorization," *Nature*, vol. 401, no. 6755, pp. 788–791, 1999.

[8] S. F. Farmer, J. Gibbs, D. M. Halliday, L. M. Harrison, L. M. James, M. J. Mayston, and J. A. Stephens, "Changes in emg coherence between long and short thumb abductor muscles during human development," *The Journal of physiology*, vol. 579, no. 2, pp. 389–402, 2007.

[9] D. Halliday, J. Rosenberg, A. Amjad, P. Breeze, B. Conway, S. Farmer, *et al.*, "A framework for the analysis of mixed time series/point process data-theory and application to the study of physiological tremor, single motor unit discharges and electromyograms," *Progress in biophysics and molecular biology*, vol. 64, no. 2, p. 237, 1995.

[10] V. von Tscharner, M. Ullrich, M. Mohr, D. C. Marquez, and B. M. Nigg, "Beta, gamma band, and high-frequency coherence of emgs of vasti muscles caused by clustering of motor units," *Experimental brain research*, vol. 236, no. 11, pp. 3065–3075, 2018.

[11] J. T. Gwin and D. P. Ferris, "Beta-and gamma-range human lower limb corticomuscular coherence," *Frontiers in human neuroscience*, vol. 6, p. 258, 2012.

[12] J. McAuley, S. Farmer, J. Rothwell, and C. Marsden, "Common 3 and 10 hz oscillations modulate human eye and finger movements while they simultaneously track a visual target," *The Journal of physiology*, vol. 515, no. 3, pp. 905–917, 1999.

[13] A. Ritterband-Rosenbaum, A. Herskind, X. Li, M. Willerslev-Olsen, M. D. Olsen, S. F. Farmer, and J. B. Nielsen, "A critical period of corticomuscular and emg–emg coherence detection in healthy infants aged 9–25 weeks," *The Journal of physiology*, vol. 595, no. 8, pp. 2699–2713, 2017.